Research Article

Corrosion Inhibition of C-steel used in Petroleum Pipelines in Aqueous Solutions using some Chalcone Derivatives

Fouda A.S[1]*, Elmorsi M.A[2], Fayed T [2] and M.Medhat[1]

[1]Department of Chemistry, Faculty of Science, El-Mansoura University, El-Mansoura-35516, EGYPT
[2]Department of Chemistry, Faculty of Science, Tanta University, Tanta, EGYPT

Abstract

The corrosion inhibition of carbon steel in HCl in the presence of chalcone derivatives was studied using weight loss, potentiodynamic polarization, electrochemical frequency modulation (EFM) and electrochemical impedance spectroscopy (EIS) techniques. The study revealed that the corrosion rate increases with temperature. Addition of chalcone derivatives to the corrodent solution lowered the corrosion rate of carbon steel. Inhibition efficiency (%IE) of chalcone derivatives was found to increase with concentration and decreased with temperature. Adsorption of chalcone molecule on carbon steel surface was found to obey the Temkin adsorption isotherm The phenomenon of physical adsorption is proposed from the obtained thermodynamic parameters.

Keywords: Chalcone derivatives, corrosion inhibition, carbon steel, HCl

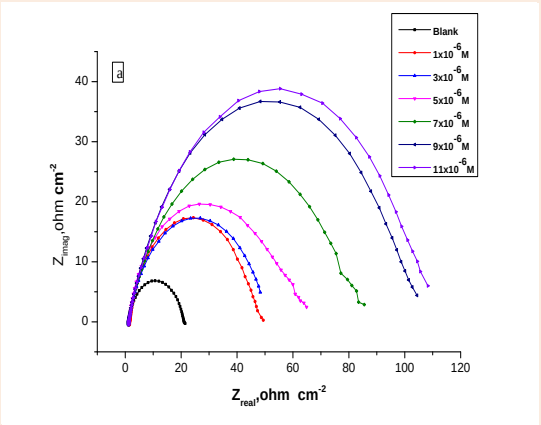

***Correspondence**
A. S. Fouda,
Email: asfouda@mans.edu.eg

Introduction

Corrosion is a fundamental process playing an important role in economics and safety, particularly for metals and alloys. Carbon steel has found wide applications in a broad spectrum of industries and machinery; despite its tendency to corrosion. Corrosion inhibition of carbon steel, therefore is a matter of theoretical as well as practical importance [1-8]. Acid solutions are widely used in industry, some of the important fields of applications being acid pickling of iron and steel, chemical cleaning and processing, ore production and oil well acidification. Because of the aggressiveness of acid solutions, inhibitors are commonly used to reduce the corrosive attack on metallic materials. Most well-known acid inhibitors are organic compounds containing nitrogen, sulfur, and oxygen atoms. However, these compounds, despite their high inhibition performance, are toxic and carcinogenic. The safety and environmental issues of corrosion inhibitors arisen in industries has always been a global concern. However, only a few non-toxic and eco-friendly compounds have been investigated as corrosion inhibitors. Among the wide chemical organic compounds are chalcone derivatives which have recently been investigated as corrosion inhibitors for various metals and alloys in acid media [9-10]. These substances generally become effective by adsorption on the metal surface. The adsorbed species protect the metal from the aggressive medium, which causes decomposition of the metal, but also on the chemical structures of the inhibitors [11-13].

Experimental procedure

Weight loss method

Materials used for the study were carbon steel sheets of composition (weight %) Mn (0.03), P (0.033), C (0.2), Si (0.14) and Fe balance. The sheet was mechanically pressed cut to form different coupons, each of dimension, 2 x 2 x

0.1 cm. Each coupon was degreased by washing with ethanol, rinsed in acetone, allowed to dry and preserved in a desiccator. All reagents used for the study were Analar grade and double distilled water was used for their preparation. Concentration of HCl used for the study was 1 M while those of chalcone derivatives (the inhibitor used) were (1–11) $x10^{-6}$ M. All the experiments were performed at room temperature for an immersion time of 3 hrs. The inhibition efficiency (% IE) and degree of surface coverage (θ) were calculated from the equation (1) [14] where, W^o and W are the weight losses without and with inhibitor, respectively.

$$\% \text{ IE} = \theta \times 100 = [(W^o - W)/ W^o] \times 100 \quad (1)$$

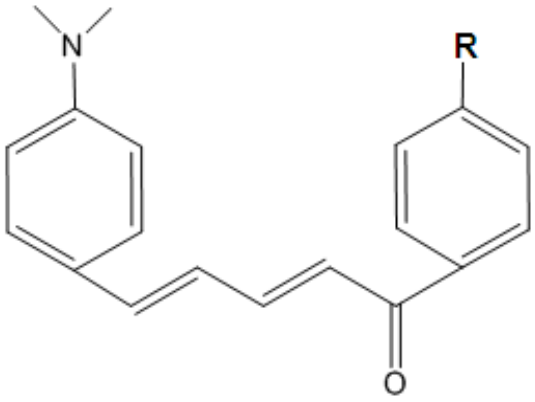

Scheme 1 Molecular structure of chalcone derivatives
[R= OCH_3 (A), =CH_3 (B), =H (C), and =Cl (D)]

The electrochemical studies were made using a three electrode cell assembly at room temperature [15-16]. The working electrode was a carbon steel of the above composition of 1 cm^2 area and the rest being covered by using commercially available lacquer. A rectangular platinum foil of 1 cm^2 was used as counter electrode and saturated calomel electrode (SCE) as reference electrode. The working electrode was abraded with different grades of emery papers (up to1200 grit size), washed with double distilled water and degreased with acetone. The polarization study was carried out from -1.0 to 0.0 V versus SCE with scan rate of 1 mV/s. The inhibition efficiency has been calculated using the relationship:

$$\% \text{ IE} = \theta \times 100 = [(i_{corr} - i_{corr(inh)}) / i_{corr}] \times 100 \quad (2)$$

Where, i_{corr} and $i_{corr(inh)}$ are the uninhibited and inhibited corrosion current densities values, respectively, determined by extrapolation of Tafel lines.

The electrochemical impedance spectroscopy (EIS), spectra were recorded at open circuit potential (OCP) after immersion the electrode for 30 min in the test solution. The signal was 5 mV peak to peak and the frequency range studied was between 100 kHz and 0.2 Hz. The inhibition efficiency (% IE) and the surface coverage (θ) of the inhibitor obtained from the impedance measurements were calculated by applying the following relation:

$$\% \text{ IE} = \Theta \times 100 = [1- (R^o_{ct} / R_{ct})] \times 100 \quad (3)$$

Where, R^o_{ct} and R_{ct} are the charge transfer resistance in the absence and presence of inhibitor, respectively. For the electrochemical frequency modulation technique (EFM), a potential perturbation by two sine waves of different frequencies is applied to the system. As a corrosion process is nonlinear in nature, responses are generated at more frequencies than the frequencies of the applied signal. The current responses can be measured at zero, harmonic, and

intermodulation frequencies. Analysis of these current responses can result in the corrosion current density and Tafel parameters. The inhibition efficiency (%IE) and the surface coverage (θ) of the inhibitor obtained from eq. (2)

All Electrochemical experiments were carried out using Potentiostat/Galvanostat/ Zra analyzer (Gamry PCI 300/4). A personal computer with EIS300 software for EIS, DC105 software for polarization and EFM140 software for EFM measurements and Echem Analyst 5.21 was used for data fitting and calculating.

Results and discussion

Weight loss measurements:

Figure 1 shows plots for the variation of weight loss with time for the corrosion of C-steel in 1M HCl containing various concentrations of compound (A) at 25°C. Similar curves were obtained for other inhibitors but not shown. From these plots, it is evident that the weight loss of C-steel was found to decrease with increase in the concentration of compound (A). The weight loss of C-steel in the blank solution was found to be higher than those obtained for solutions containing various concentrations of compound (A). This indicates that compound (A) is an inhibitor for the corrosion of C-steel. In **Table 1**, values of the corrosion rates of C-steel and inhibition efficiency of all studied compounds in HCl are presented. The degree of surface coverage (θ) and inhibition efficiency (% IE) were calculated using equation (4):

$$\% IE = \theta \times 100 = [1-CR_{inh}/ CR_{free}) \times 100 \quad (4)$$

Where, CR_{inh} and CR_{free} are the corrosion rates in the absence and presence of inhibitor, respectively.

It can be seen that the maximum of 84.22% inhibition efficiency is achieved at 11 x 10^{-6}M of inhibitor concentration and %IE increases with increasing the inhibitors concentrations[17] and the order of the inhibition efficiency of inhibitors was as follows: A > B > C > D.

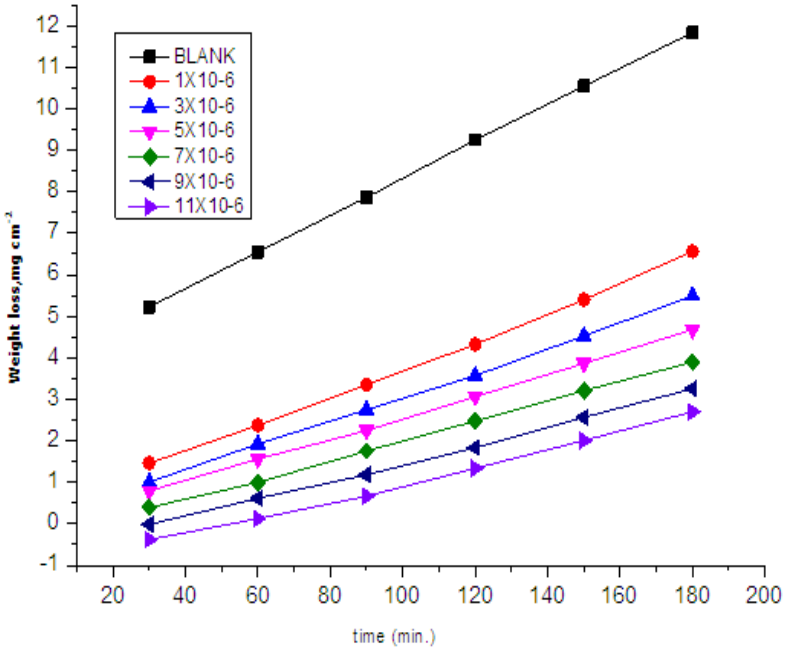

Figure 1 Weight loss-time curves for C-steel dissolution in 1 M HCl in the absence and presence of different concentrations of chalcone (A) at 25°C

Table 1 Values of the corrosion rates of C-steel and inhibition efficiency of all studied compounds in HCl

Conc.,x 10^6 M	A		B		C		D	
	%IE	C.R. x10^2 mg cm^{-2} min^{-1}	%IE	C.R. x10^2 mg cm^{-2} min^{-1}	%IE	C.R. x10^2 mg cm^{-2} min^{-1}	%IE	C.R. x10^2 mg cm-2 min^{-1}
1	53.3	3.60	48.5	4.08	44.8	5.06	40.7	7.71
3	66.5	2.58	61.9	3.02	58.10	3.85	52.9	6.13
5	73.1	2.07	68.5	2.49	64.3	3.27	59.7	5.25
7	77.6	1.73	73.0	2.14	68.9	2.85	64.2	4.66
9	81.3	1.44	76.2	1.88	72.0	2.56	67.5	4.24
11	84.2	1.11	78.8	1.68	74.7	2.32	69.8	3.92

Effect of temperature on inhibition efficiency (% IE):

The inhibition efficiencies (% IE) of C-steel corrosion in the presence of various concentrations of the investigated chalcone derivatives and at different temperatures were calculated and are listed in **Table 2.** The results of Table-2 illustrate the variation of corrosion rate (C.R.) and % IE with inhibitors concentrations at different temperatures. The obtained data revealed that, the inhibition efficiency decreased with an increase in the inhibitor concentration. This suggests that the inhibitor species are adsorbed on the C-steel /solution interface where the adsorbed species mechanically form a protected film on the metal surface which inhibits the action of the corrosion. A close comparison between Tables 2 and 3 revealed that weight loss of C-steel increases with increasing temperature indicating that the rate of corrosion of C-steel increases with increase in temperature. The value of inhibition efficiency was decreased with rise in temperature suggests that physical adsorption mechanism [18]. These results indicate that the adsorption of investigated compounds shield the metal surface at room temperature [19]. However, it may be de- shielded from the surface with rise in temperature.

Table 2 Variation of inhibition efficiency (%IE) and corrosion Rate (C.R.) for various concentrations of the studied inhibitors at different temperatures

Temp. °C	Conc.x 10^6 M	A		B		C		D	
		% IE	C.R.x x10^2 mg cm^{-2} min^{-1}	% IE	C.R.x10^2 mg cm^{-2} min^{-1}	% IE	C.R.x10^2 mg cm^{-2} min^{-1}	%IE	C.R.x10^2 mg cm^{-2} min^{-1}
30	1	52.8	6.26	47.9	7.12	44.2	9.08	39.6	13.01
	3	63.3	4.87	59.5	5.54	56.1	7.14	50.2	10.73
	5	68.5	4.17	64.5	4.85	61.8	6.22	55.5	9.59
	7	71.8	3.74	67.9	4.38	65.4	5.63	59.5	8.73
	9	74.4	3.39	70.8	3.99	68.1	5.18	62.7	8.04
	11	76.4	3.15	72.6	3.47	70.2	4.84	64.8	7.58
35	1	50.1	6.85	44.7	7.90	42.4	10.12	39.2	15.70
	3	61.5	5.29	56.3	6.25	53.7	8.14	48.6	13.28
	5	66.8	4.56	61.9	5.45	58.6	7.28	53.6	12.00
	7	70.7	4.03	66.0	4.86	62.5	6.59	56.9	11.13
	9	73.4	3.65	68.8	4.46	65.8	6.01	59.9	10.36
	11	75.7	3.33	71.0	4.14	68.3	5.58	62.0	9.81
40	1	49.5	7.12	44.6	8.10	41.4	10.62	37.6	15.50
	3	60.7	5.54	54.8	6.62	51.7	8.76	47.4	13.06
	5	65.8	4.82	60.1	5.84	56.5	7.88	51.5	12.04
	7	69.8	4.32	63.8	5.30	59.8	7.28	54.5	11.30

	9	72.0	3.94	66.6	4.89	62.4	6.82	56.5	10.81
	11	74.3	3.62	68.9	4.55	64.3	6.46	58.3	10.37
45	1	47.1	7.72	42.1	9.12	38.7	12.45	37.1	23.45
	3	59.1	5.96	53.6	7.31	49.8	10.18	45.6	20.23
	5	64.9	5.12	59.9	6.32	55.6	9.02	51.2	18.34
	7	68.7	4.57	62.4	5.92	54.9	8.24	52.8	17.56
	9	71.4	4.17	64.1	5.65	68.6	7.95	54.8	16.81
	11	73.7	3.83	65.1	5.49	62.3	7.65	56.5	16.20

Adsorption isotherms:

Organic molecules like inhibitor molecules inhibit the corrosion process via their adsorption on metal surface. Theoretically, the adsorption process can be regarded as a single substitutional process in which an inhibitor molecule, $I_{inh.}$, in the aqueous phase substitutes an "x" number of water molecules adsorbed on the metal surface [20] vis,

$$I_{inh\ (aq)} + x\ H_2O_{\ (sur)} \rightarrow I_{inh\ (sur)} + x\ H_2O_{\ (aq)} \quad (5)$$

Where x is known as the size ratio and simply equals the number of adsorbed water molecules replaced by a single inhibitor molecule. The adsorption depends on the structure of the inhibitor, the type of the metal and the nature of its surface, the nature of the corrosion medium and its pH value, the temperature and the electrochemical potential of the metal-solution interface. Also, the adsorption provides information about the interaction among the adsorbed molecules themselves as well as their interaction with the metal surface. Actually an adsorbed molecule may make the surface more difficult or less difficult for another molecule to become attached to a neighboring site and multilayer adsorption may take place. There may be more or less than one inhibitor molecule per surface site. Finally, various surface sites could have varying degrees of activation. For these reasons a number of mathematical adsorption isotherm expressions have been developed to take into consideration some of non-ideal effects. Adsorption isotherm equations are generally of the form [21]:

$$f(\theta, x) \exp(-a, \theta) = KC \quad (6)$$

Where f (θ, x) is the configurational factor that depends essentially on the physical model and assumptions underlying the derivation of the isotherm 'a' is a molecular interaction parameter depending upon molecular interactions in the adsorption layer and the degree of heterogeneity of the surface. All adsorption expressions include the equilibrium constant of the adsorption process, K, which is related to the standard free energy of adsorption ($\Delta G^{o}_{ads.}$) by:

$$K = 1/55.5 \exp(-\Delta G^{o}_{ads} / RT) \quad (7)$$

Where R is the universal gas constant and T is the absolute temperature. A number of mathematical relationships for the adsorption isotherms have been suggested to fit the experiment data of the present work. The simplest equation is that due to Temkin and is given by the general equation:

$$\text{In } K\ C = a\ \theta \quad (8)$$

Where K is the equilibrium constant of the adsorption reaction; C is the inhibitor concentration in the bulk of the solution; a is the interaction parameter and θ is the surface coverage. The surface coverage i.e. the fraction of the surface is covered by the inhibitor molecules.

Plots of θ vs.log C (Temkin adsorption plots) for adsorption of inhibitors on the surface of C-steel in 1M HCl solution at 25°C are shown in **Figure 2**. The data gave straight lines indicating that Temkin's isotherm is valid for

these systems. Temkin's isotherm is applied for ideal case of physical and chemical adsorption on a smooth surface with no interaction between the adsorbed molecules.

On the other hand, it is found that the kinetic-thermodynamic model of El Awady et al [22]:

$$\text{Log } (\theta / (1-\theta)) = \log K' + y \log C \quad (9)$$

It is valid to operate the present adsorption data. The equilibrium constant of adsorption $K=K'^{(1/y)}$, where 1/y is the number of the surface active sites occupied by one inhibitors molecule and C is the bulk concentration of the inhibitor. The calculated values of 1/y, K and ΔG°_{ads} are given in **Table 3.** Inspection of the data of these Tables shows that the large values of ΔG^{o}_{ads} and its negative sign, indicate that the adsorption of inhibitors additives on the C-steel surface is proceeding spontaneously and is accompanied by a highly-efficient adsorption. It is worth noting that the value of 1/y is more than unity. This means that the given inhibitor molecules will occupy more than one active site. In general, the values of ΔG^{o}_{ads} were obtained from El-Awady et al model are comparable with those obtained from Temkin's isotherm.

Table 3 Parameters from Temkin isotherm and kinetic model models for C-steel in 1 M HCl for investigated compounds

Compound	Temkin			Kinetic model		
	a	K_{ads} x10^4 M^{-1}	$-\Delta G^{o}_{ads}$ kJ mol^{-1}	1/y	K_{ads} x10^6 M^{-1}	$-\Delta G^{o}_{ads}$, kJ mol^{-1}
A	4.8	6.4	37.4	1.6	1.1	40.4
B	4.9	5.7	37.1	1.8	0.84	38.8
C	5.0	5.2	36.9	1.9	0.64	37.1
D	4.9	2.9	35.4	2.0	0.45	36.2

From these results it may be generalized that the more efficient inhibitor has more negative ΔG^{o}_{ads} value so that from the tabulated values of ΔG^{o}_{ads} the order of inhibition efficiency is as follows: A > B > C > D

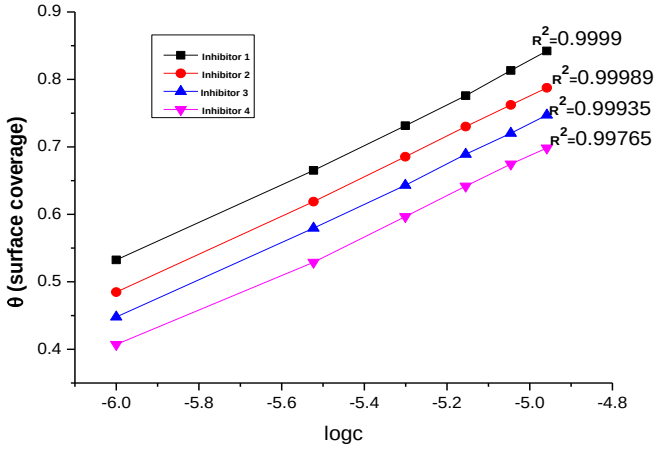

Figure 2 Temkin adsorption isotherm as (θ) vs log C of investigated compounds for the corrosion of C-steel in 1 M HCl solution at 25°C

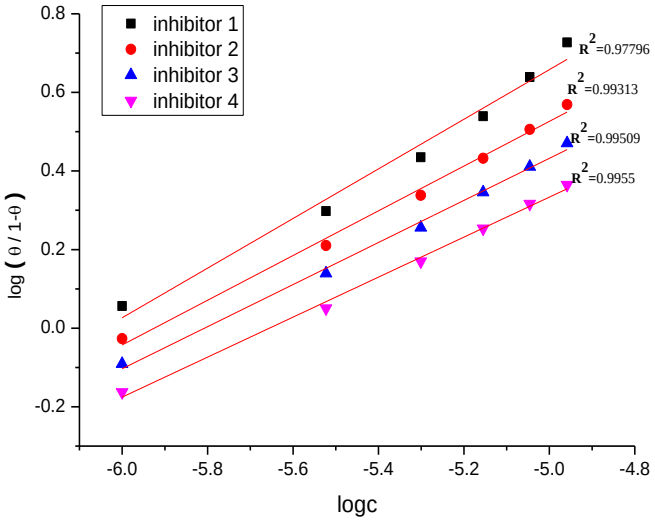

Figure 3 Kinetic model isotherm curves for the dissolution of C-steel in the presence of different concentrations of investigated compounds in 1 M HCl solution at 25°C

Activation parameters of corrosion process

The corrosion rate of C-steel in the absence and presence of inhibitors obeys Arrhenius type equation as it increases with raising solution temperature. The dependence of corrosion rate (k_{corr}) on the temperature can be expressed by Arrhenius equation 5:

$$k_{corr} = A \exp (-E_a^*/ RT) \quad (9)$$

Where, A is the pre-exponential factor and E^*_a is the apparent activation energy of the corrosion process. Arrhenius plot obtained for the corrosion of carbon steel in 1 M HCl acid solutions in the presence of different concentrations of compound (A) is shown in **Figure 4.** E^*_a values determined from the slopes of these linear plots are shown in **Table 4.** The linear regression (R^2) is close to 1 which indicates that the corrosion of C-steel in 1 M HCl solutions can be elucidated using the kinetic model. Table-4 showed that the values of E^*_a for inhibited solution is higher than that for uninhibited solution, suggesting that dissolution of C-steel is slow in the presence of inhibitor. It is known from Eq. 9 that the higher E_a^* values lead to the lower corrosion rate. This is due to the formation of a film on the carbon steel surface serving as an energy barrier for the carbon steel corrosion [23].

Enthalpy and entropy of activation (ΔH^*, ΔS^*) of the corrosion process were calculated from the transition state theory as given from equation 10 **(Table 4):**

$$k_{corr} = (RT/ Nh) \exp (\Delta S^*/R) \exp (-\Delta H^*/RT) \quad (10)$$

Where, h is Planck's constant and N is Avogadro's number. A plot of log (k_{corr}/ T) vs. 1/ T for carbon steel in 1 M HCl with different concentrations of compound (A) gives straight lines as shown in **Figure 5.**

Similar curves were obtained for other compounds but not shown. Values of ΔH^* are positive. This indicates that the corrosion process is an endothermic one. The entropy of activation ΔS^* is large and negative. This implies that the activated complex represents association rather than dissociation step, indicating that a decrease in disorder takes place, going from reactants to the activated complex [24].

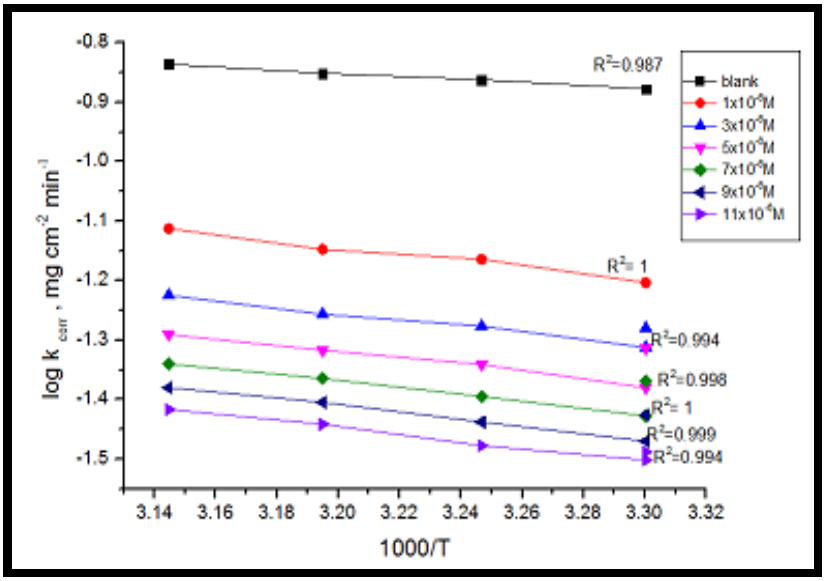

Figure 4 Arrhenius plots for C-steel rates (k_{corr}) after 120 min. immersion in 1 M HCl in the absence and presence of various concentrations of inhibitor (A)

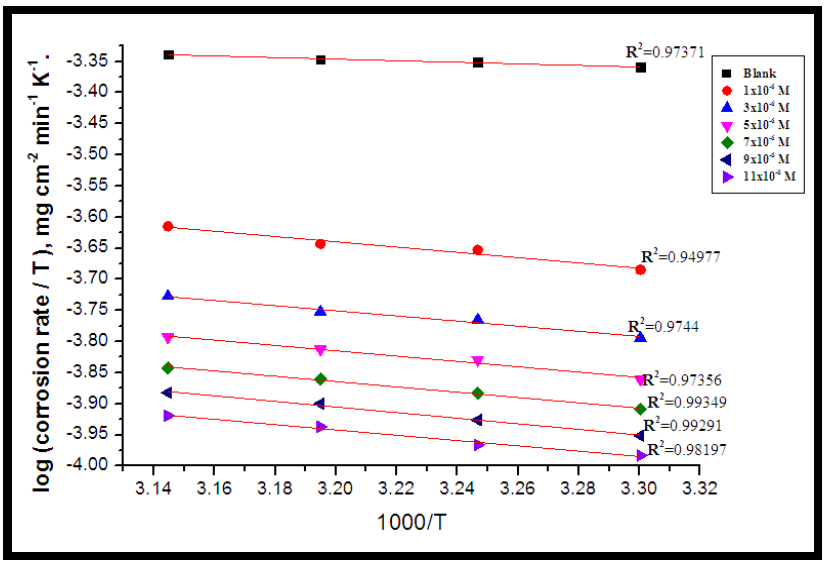

Figure 5 Transition state plots for C-steel (k_{corr}/ T vs 1/T) after 120 min. immersion in 1 M HCl in the absence and presence of various concentrations of inhibitor (A)

From the results of **Table 4,** it is clear that the addition of the inhibitor modified the values of the apparent activation energies. It was found that values of E_a^* for inhibited systems in the acid media increased with increasing concentration of inhibitor which was higher than those for uninhibited system. This was indicative of higher energy barrier formed by the organic compounds towards the corrosion reaction [25]. The E_a^* values are helpful to determine the type of adsorption. In the case of chemisorption, the E_a^* values are greater than 80 kJ mol^{-1} where as in this case of chemisorption they are lesser than 80 kJ mol^{-1} [26]. This suggests that a physical mode of adsorption had occurred due to the interaction between the organic compounds and C-steel surface [27-34] and the organic derivatives are sensitive to reaction temperatures [35]. From the above discussion, it is clear that the addition of organic compounds

modified the values of E_a^* which is due to adsorption [36, 37] on C-steel surface through chloride. This leads to the formation of species of the kind [$FeCl^-$…… organic derivative$^+$]$_{ads}$ which then inhibit the anodic dissolution of C-steel, supporting the physisorption mechanism. On the other hand, chemisorption which arises due to the interaction of aromatic rings, nitrogen and oxygen atoms with Fe present in C-steel cannot be ignored.

The positive signs of ΔH^* reflect the endothermic nature of the carbon steel dissolution process. Large and negative values of ΔS^* imply that the activated complex in the rate-determining step represents an association rather than dissociation step, meaning that decrease in disordering takes place on going from reactants to the activated complex [38-42]. The order of the inhibition efficiencies of organic derivative derivatives as gathered from the increase in E_a^* and ΔH^* values and decrease in ΔS^* values are as follows: A > B > C > D

Table 4 Activation parameters of the dissolution of C-steel in 1 M HCl in the absence and presence of different concentrations of chalcone derivatives

Inhibitor	Conc., M.	Activation parameters		
		E_a^*	ΔH^*	$-\Delta S^*$
		kJ mol^{-1}	kJ mol^{-1}	J mol^{-1} K^{-1}
HCl	0.0	5.02	4.61	253.91
D	1×10^{-6}	5.87	7.12	241.28
	3×10^{-6}	6.45	7.87	244.19
	5×10^{-6}	6.64	8.19	244.42
	7×10^{-6}	7.01	8.98	245.41
	9×10^{-6}	8.38	9.61	246.81
	11×10^{-6}	9.73	10.15	247.11
C	1×10^{-6}	15.06	9.71	234.97
	3×10^{-6}	16.05	11.68	235.53
	5×10^{-6}	16.11	12.27	237.96
	7×10^{-6}	16.49	13.29	243.26
	9×10^{-6}	19.76	15.61	245.45
	11×10^{-6}	23.41	17.34	246.34
B	1×10^{-6}	26.33	13.34	210.91
	3×10^{-6}	26.96	15.64	215.43
	5×10^{-6}	27.45	16.57	220.43
	7×10^{-6}	28.01	17.34	231.69
	9×10^{-6}	28.61	20.03	240.59
	11×10^{-6}	29.34	21.76	245.53
A	1×10^{-6}	48.02	25.42	178.39
	3×10^{-6}	49.74	27.52	200.65
	5×10^{-6}	50.27	28.54	210.57
	7×10^{-6}	52.88	34.72	219.77
	9×10^{-6}	55.18	36.82	233.55
	11×10^{-6}	56.45	38.02	240.12

Potentiodynamic Polarization Measurements

Polarization measurements were carried out in order to gain knowledge concerning the kinetics of the cathodic and anodic reactions. **Figure 6** presents the results of the effect of compound (A) on the cathodic and anodic polarization curves of C- steel in 1 M HCl. Similar curves for other compounds were obtained but not shown. It could be observed that both the cathodic and anodic reactions were suppressed with the addition of investigated compounds, which suggested that these compounds reduced anodic dissolution and also retarded the hydrogen evolution reaction. Electrochemical corrosion kinetics parameters, i.e. corrosion potential (E_{corr}), cathodic and anodic Tafel slopes (β_a, β_c) and corrosion current density (i_{corr}) obtained from the extrapolation of the polarization curves, were given in **Table 5.** The parallel cathodic Tafel curves in figure-6 suggested that the hydrogen evolution is activation-controlled and the reduction mechanism is not affected by the presence of the inhibitor. The region between linear part of cathodic and anodic branch of polarization curves becomes wider as the inhibitor is added to the acid solution. Similar results were found in the literature [43]. The values of β_a and β_c changed slightly with increasing inhibitor concentration indicated the influence of these compounds on the kinetics of metal dissolution and of hydrogen evolution. Due to the presence of some active sites, such as aromatic rings, hetero-atoms in the studied compounds for making adsorption, they may act as adsorption inhibitors. Being absorbed on the metal surface, these compounds controlled the anodic and cathodic reactions during corrosion process, and then their corrosion inhibition efficiencies are directly proportional to the amount of adsorbed inhibitor. The functional groups and structure of the inhibitor play important roles during the adsorption process. On the other hand, an electron transfer takes place during adsorption of the neutral organic compounds at metal surface [44]. As it can be seen from **Table 5**, the studied inhibitor reduced both anodic and cathodic currents with a slight shift in corrosion potential (47 mV). According to Ferreira and others [45], if the displacement in corrosion potential is more than 85mV with respect to corrosion potential of the blank solution, the inhibitor can be seen as a cathodic or anodic type. In the present study, the displacement was 47 mV which indicated that the studied inhibitor is mixed- type inhibitor. The results obtained from Tafel polarization showed good agreement with the results obtained from weight loss method. The surface coverage (θ) and % IE were calculated using equation 11.

$$\%IE = \theta \times 100 = [1-(i_{corr}/i°_{corr})] \times 100 \qquad (11)$$

Where i_{corr} and $i°_{corr}$ are the current densities in presence and absence of inhibitor, respectively.

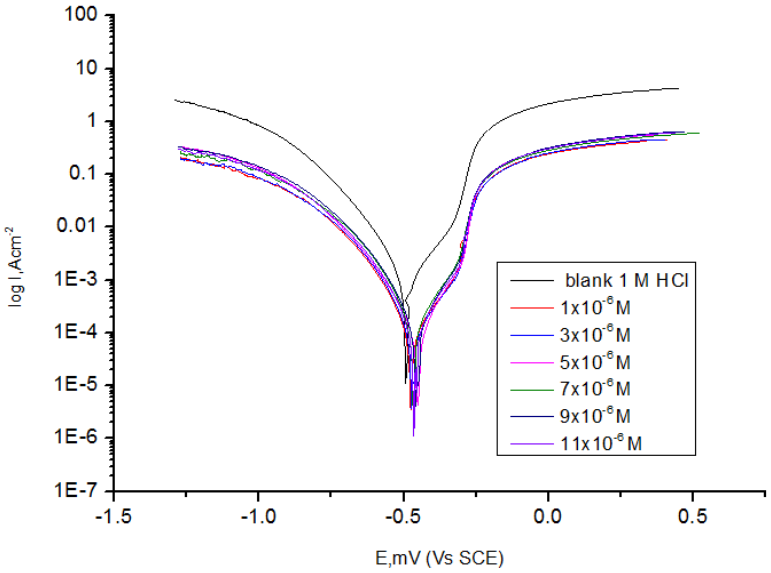

Figure 6 Potentiodynamic polarization curves for the dissolution of carbon steel in 1 M HCl in the absence and presence of different concentrations of compound (A) at 25ºC

Table 5 The effect of concentrations of investigated compounds on the free corrosion potential (E_{corr}), corrosion current density (i_{corr}), Tafel slopes (β_c, β_a), corrosion rate (k_{corr}), inhibition efficiency (% IE) and degree of surface coverage (θ) of carbon steel in 1 M HCl at 25ºC

Inhibitor	Conc.x10^6 M	-E_{corr} mVvs SCE	i_{corr} µA cm^{-2}	β_a mV dec^{-1}	β_c mV dec^{-1}	k_{corr} mmy^{-1}	θ	%IE
blank	- -	492	615	108.8	169.9	280.9	- -	- -
A	1	475	180	198.5	151.6	82.1	0.707	70.7
	3	471	179	213.6	167.3	81.8	0.709	70.9
	5	452	130	126.8	153.6	59.3	0.789	78.9
	7	467	111	111	154	50.5	0.820	82.0
	9	457	77.9	94.9	118.5	35.6	0.873	87.3
	11	465	74	106.8	128.7	33.8	0.880	88.0
B	1	504	200	248.7	223.7	91.2	0.675	67.5
	3	511	192	322.5	166.9	87.5	0.688	68.8
	5	497	188	285.1	161.1	85.8	0.694	69.4
	7	512	125	186.1	117	56.9	0.797	79.7
	9	501	90.4	155.8	187.6	41.3	0.853	85.3
	11	505	77.9	159.8	218.5	35.6	0.873	87.3
C	1	473	252	201.0	192.8	115.1	0.590	59.0
	3	497	220	344.6	172.2	100.6	0.642	64.2
	5	471	197	151.3	182.1	90.1	0.680	68.0
	7	491	140	190.3	158.8	64.1	0.772	77.2
	9	478	129	114.6	158.5	58.8	0.790	79.0
	11	476	109	139.4	152.2	49.6	0.820	82.0
D	1	465	263	113.9	192.4	120.1	0.572	57.2
	3	483	245	116.3	216.9	112.2	0.602	60.2
	5	456	200	104.6	174.6	91.3	0.675	67.5
	7	459	152	103.3	189.3	69.6	0.753	75.3
	9	456	131	139.5	208.0	59.7	0.787	78.7
	11	466	123	92.5	171.7	56.0	0.800	80.0

Electrochemical impedance spectroscopy (EIS) measurements

The corrosion of C-steel in 1 M HCl in the presence and absence of the investigated chalcone derivatives was investigated by EIS method at 25ºC after 30 min immersion. Nyquist plots in the absence and presence of investigated compounds are presented in **Figure-7,** also Bode plots are presented in **Figure-8.** It is apparent that Nyquist plots show a single capacitive loop, both in uninhibited and inhibited solutions. The impedance data of C-steel in 1 M HCl are analyzed in terms of an equivalent circuit model **(Figure-9)** which includes the solution resistance, R_s, and the double layer capacitance, C_{dl}, which is placed in parallel to the charge transfer resistance R_{ct}[46] due to the charge transfer reaction. For the Nyquist plots it is obvious that low frequency data are on the right side of the plot and higher frequency data are on the left. This is true for EIS data where impedance usually falls as frequency rises (this is not true for all circuits). The capacity of double layer (C_{dl}) can be calculated from the following equation:

$$C_{dl} = 1/2\pi f_{max} Rct \qquad (12)$$

Where, f_{max} is the maximum frequency. The parameters obtained from impedance measurements are given in **Table 6.** It can see from **Table 6** that the values of charge transfer resistance Rct increase with chalcone concentration [47].

In the case of impedance studies, % IE increases with chalcone concentration. It is also noted that the C_{dl} values tend to decrease when the concentration of chalcone increases. This decrease in C_{dl}, which can result from a decrease in local dielectric constant and/or an increase in the thickness of the electrical double layer, suggests that this chalcone molecules function by adsorption at the metal/solution interface [48]

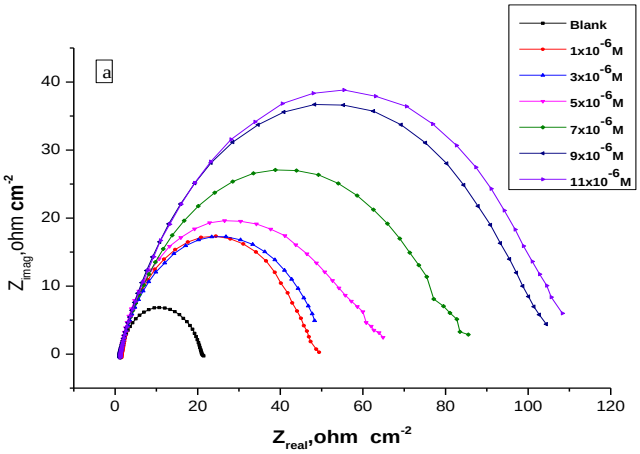

Figure 7 Nyquist plots for carbon steel in 1 M HCl solutions in the absence and presence of various concentrations of inhibitor (A) at 25ºC

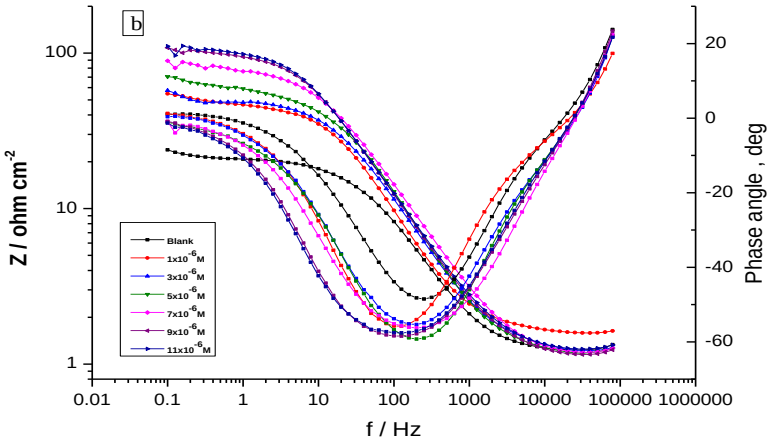

Figure 8 Bode plots for carbon steel in 1 M HCl solutions in the absence and presence of various concentrations of inhibitor (A) at 25ºC

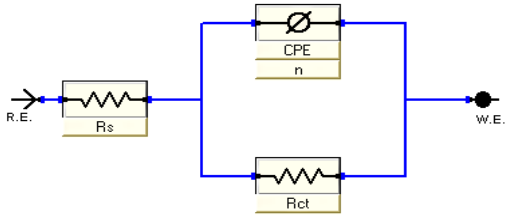

Figure 9 Equivalent circuit model used to fit the impedance spectra

Table 7 Electrochemical kinetic parameters obtained by EIS technique for the corrosion of carbon steel in 1 M HCl at different concentrations of inhibitor (A) at 25º C

Inhibitor	Conc.x10^6 M	C_{dl} μF cm^{-2}	R_{ct} Ω cm^2	θ	% IE
Blank	0.0	212.52	19.83	- -	- -
A	1	231.20	47.11	0.579	57.9
	3	229.25	49.02	0.596	59.6
	5	227.15	59.37	0.666	66.6
	7	190.09	80.89	0.755	75.5
	9	174.68	102.9	0.807	80.7
	11	173.39	107.0	0.815	81.5
B	1	251.61	38.14	0.479	47.9
	3	237.68	47.13	0.579	57.9
	5	229.28	53.80	0.632	63.2
	7	227.02	70.18	0.717	71.7
	9	185.53	80.86	0.755	75.5
	11	174.45	102.9	0.807	80.7
C	1	251.74	33.83	0.414	41.4
	3	240.45	38.12	0.481	48.1
	5	237.51	47.08	0.579	57.9
	7	229.24	53.81	0.631	63.1
	9	185.52	70.16	0.718	71.8
	11	174.78	80.88	0.755	75.5
D	1	240.44	26.48	0.251	25.1
	3	237.69	33.85	0.414	41.4
	5	229.13	38.12	0.481	48.1
	7	185.45	47.12	0.579	57.9
	9	173.73	59.36	0.666	66.6
	11	153.77	70.24	0.718	71.8

Electrochemical Frequency Modulation (EFM) Measurements

In corrosion research, it is known that the corrosion process is non-linear in nature, a potential distortion by one or more sine waves will generate responses at more frequencies than the frequencies of applied signal. Virtually no attention has been given to the intermodulation or electrochemical frequency modulation. However, EFM showed that this non-linear response contains enough information about the corroding system so that the corrosion current can be calculated directly. Electrochemical frequency modulation (EFM) is non-destructive corrosion measurement technique that can directly give values of corrosion current without prior knowledge of Tafel constants. In this technique current responses due to a potential perturbation by one or more sine waves are measured at more frequencies than the frequency of the applied signal, for example at zero harmonic and intermodulation frequencies. The great strength of the EFM is the causality factors which serve as an internal check on the validity of the EFM measurement. The results of EFM experiments are a spectrum of current response as a function of frequency. The

spectra contain current responses assigned for harmonical and intermodulation current peaks. The results of EFM experiments are a spectrum of current response as a function of frequency. The spectrum is called the intermodulation spectrum and examples for the absence and presence of $1x10^{-6}$ M of chalcone derivative to 1 M HCl solution for C-steel are shown in **Figures 10** and **11,** respectively. The larger peaks were used to calculate the corrosion current density (icorr), the Tafel slopes (β_c and β_a) and the causality factors (CF-2 and CF-3). These electrochemical parameters were simultaneously determined and are listed in **Table 8.** As it can be seen from this Table the corrosion current density decreases in the presence of cefixime than in its absence. The causality factors also indicate that the measured data are of good quality.

Table 8 Electrochemical kinetic parameters obtained by EFM technique for carbon steel in 1 M HCl solutions with different concentrations of chalcone derivatives

Inh	Conc., $x10^{-6}$M	i_{corr} µA cm^{-2}	β_a, mV dec^{-1}	β_c mV dec^{-1}	CF-2	CF-3	θ	% IE
	- ----	765.2	33	42	1.66	2.36	----	----
A	1	292.4	33	37	1.71	2.31	0.618	61.8
	3	252.4	32	72	2.18	3.13	0.670	67.0
	5	191.1	93	111	1.94	2.35	0.750	75.0
	7	159.4	131	18	1.93	2.99	0.792	79.2
	9	95.75	59	73	1.9	2.79	0.875	87.5
	11	92.65	98	110	1.82	2.87	0.879	87.9
B	1	380.1	88	92	1.06	2.45	0.503	50.3
	3	275.9	27	39	2.43	3.21	0.639	63.9
	5	253.0	25	32	2.10	3.50	0.669	66.9
	7	236.2	96	107	1.82	2.64	0.691	69.1
	9	218.2	101	114	1.87	2.25	0.715	71.5
	11	197.2	99	104	2.18	2.39	0.742	74.2
C	1	407.7	51	71	1.34	2.36	0.467	46.7
	3	309.2	79	108	1.88	2.99	0.596	59.6
	5	288.9	93	106	1.71	3.01	0.622	62.2
	7	248	98	112	1.97	3.09	0.676	67.6
	9	245.9	97	105	2.06	3.15	0.679	67.9
	11	232.8	105	126	2.09	3.33	0.696	69.6
D	1	488.2	92	99	1.69	2.95	0.362	36.2
	3	402	50	70	1.33	2.38	0.475	47.5
	5	377.2	86	96	2.07	2.72	0.507	50.7
	7	373.3	42	60	1.46	2.58	0.512	51.2
	9	336.6	88	102	2.04	3.01	0.560	56.0
	11	308.6	96	118	1.97	3.06	0.597	59.7

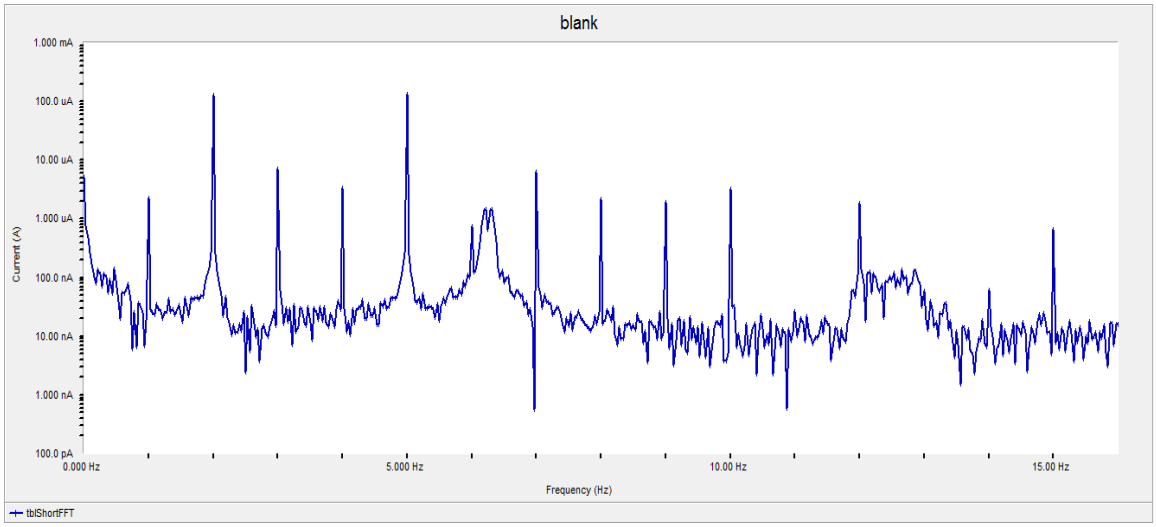

Figure 10 Intermodulation spectrum for carbon steel in 1 M HCl solutions without inhibitor at 25ºC

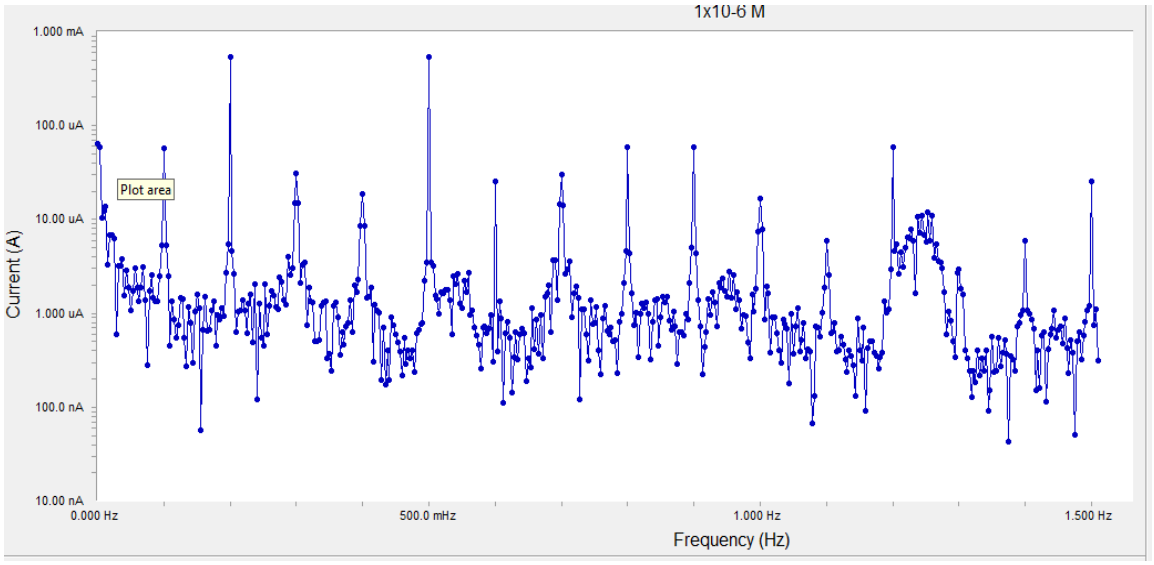

Figure 11 Intermodulation spectrum for carbon steel in 1 M HCl solutions with 1 x10^{-6} M inhibitor at 25ºC

Mechanism of Corrosion Inhibition

An elucidation of inhibition mechanism requires elaborated knowledge of the fundamental interaction amongst the protective compound and the metal surface. Many of the organic corrosion inhibitors have at least one polar unit with atoms of nitrogen, sulphur, oxygen and in some cases phosphorous. It has been reported that the inhibition efficiency increases in the order to O < N < S < P. The polar unit is considered as the reaction center for the chemisorption process. Moreover; the size, orientation, shape and electric charge on the molecule determine the degree of adsorption and therefore; the effectiveness of inhibitor. Increase in inhibition efficiencies with the increase of concentration of chalcone derivatives shows that the inhibition action is due to adsorption on the carbon steel surface. Following are the types of adsorption that may take place at metal/solution interface: (a) Electrostatic attraction between the charged molecules and charged metal (b) Interaction of unshared electron pairs in the molecule with the metal (c) Interaction of p- electrons with the metal (d) Combination of (a) and (c). In acidic solution, chalcone can be

protonated easily. Physical adsorption may take place due to electrostatic interaction between protonated molecule and the metal. Co-ordinate covalent bond formation between electron pairs of unprotonated atoms and metal surface can take place. In addition, chalcone molecule is chemically adsorbed due to interaction of π-orbitals with metal surface. In the present study, the value of ΔG^{o}_{ads} is –30 kJ mol –1, hence, showing that adsorption of chalcone molecules on the surface of carbon steel take place through both physical as well as chemical process. Nevertheless, it is clear from the results of effect of temperature that the IE values decreased at higher temperatures, thus, suggested that adsorption of chalcone does not favor at higher temperatures. It indicates that chalcone adsorbed predominantly by physical adsorption on carbon steel surface.

Conclusions

In this study, corrosion inhibition efficiency of chalcone derivatives on carbon steel in 1 M HCl was determined by chemical and electrochemical measurements. Electrochemical impedance spectroscopy data reveals increase in Rct values, which accounted for good inhibition efficiency. The polarization studies showed that these compounds behave as mixed type inhibitors. These compounds adsorbed on carbon steel surface followed Temkin adsorption isotherm.

References

[1] Z. Wahbi, A. Guenbour, H. Abou El Makarim, A. Ben Bachir and S. El Hajjaji, Porg.Org. Coat. 60(2007) 224.
[2] K.F. Khaled, Electrochim. Acta, 53(2008) 3484.
[3] K.F. Khaled, Appl. Surf. Sci., 252(2006) 4120.
[4] M.A. Amin, S.S. Abd El Rehim and H.T.M. Abdel-Fatah, Corros. Sci., 51(2009) 882.
[5] S.S. Abdel Rehim, O.A. Hazzazi, M.A. Amin and K.F. Khaled, Corros. Sci., 50(2008) 2258.
[6] H.H. Hassan, E. Abdelghani, M. A. Amin, Electrochim. Acta, 52(2007) 6359.
[7] M.A. Amin, S.S. Abd El Rehim, E.E.F. El-Sherbini and R.S. Bayoumi, Electrochim. Acta, 52(2007) 3588.
[8] K.F. Khaled, M.A. Amin, Corros. Sci., 51(2009) 1964.
[9] A. Ganesan, K. Kuppusamy, S.V. Shanmuga, G. Mayakrishnan and R. Arumugam., Ionics, 19(2013) 919
[10] A.S. Fouda, A.A. El-Shafie and H.S.Gadow. Port. Electrochim.Acta, 20(2002) 13
[11] C. Kustu, K.C. Emregul and O. Atakol, Corros.Sci. 49(2007) 2800.
[12] A.S. Fouda, M.A. Elmorsi and A. El-mekkawy, Afr. J. Pure Appl. Chem., 7(2013) 337-349.
[13] M. Behpour, S.M. Ghoreishi, M. Salavati Niasari and B. Ebrahimi, Mater. Chem. Phys., 107(2008) 153- 157.
[14] A.K.Singh; M.A. Quraishi, Corros.Sci. 52(4) (2010) 1529
[15] P.C. Pandey, R.J.Prakash, Electrochem.Soc. 145(12) (1998) 4103.
[16] J.Mohan; S.Joshi; R.Prakash; R.C. Srivastava, Electroanalysis, 16(7) (2004) 572
[17] A.Zaafarany; M.Abdallah, Inter.J.Electrochem.Sci. 5(2010) 18
[18] P.O. Ameh; N.O Eddy., 0.1 M HCl, Res.Chem.Intermediates, 1-9(2013)
[19] A Petchiammal, R.P. J.S. Deepa Selvara and K.Kalirajan, Res.J.Chem.Sci. 2(4)(2012) 24
[20] T. Paskossy; J. Electroanal. Chem., 364 (1994) 111.
[21] E. Khamis, M. A. Ameer, N.M. Al-Andis and G. Al-Senani, Corrosion, 56(2001) 27.
[22] Y. A. El-Awady, A. I. Ahmed, J. Ind. Chem., 24(1985) 601
[23] A. S Fouda., A. A. Al-Sarawy and E.E El-Katori, Desalination, 201(2006) 1
[24] G.Gece, Corros. Sci., 50(2008)2981
[25] R. Gasparac, C. R. Martin and E. Stupinisek-Lisac, J. Electrochem. Soc., 147(2) (2000) 548.
[26] A. Popova, E. Sokolova, S. Raicheva and M. Chistov, Corros. Sci., 45(2003) 33.
[27] B. B. Damaskin, Adsorption of Organic Compounds on Electrodes, Plenem Press, New York, (1971).
[28] E. E. Ebenso, U. F. Ekpe, B. I. Ita, O. E. Offiong and U. J. Ibak, Mater.Chem.Phys., 60(1999) 79.
[29] Lj.M. Vraj car and D.M. Dracgije, Corros.Sci. 44(2002) 1669.
[30] A. Dadgarnezhad, I. Sheikhshoaie and F. Baghaei, Anti-Corros. Meth. Mater, 51(4) (2004) 266.
[31] E. E. Oguzie, Pig. Res. Tech., 35(6) (2006) 334.
[32] Z. S. Smialoska and Gwieczorek, Corros. Sci., 11(1971) 843.

[33] E. E. Oguzie, A. I. Onuchukwce, P. C. Okafor and E. E. Ebenso, Pig. Res. Tech., 35(2) (2006) 63.
[34] P. K. Gosh, D. K. Guhasarkar and V. S. Gupta, Br. Corros. J., 18(4) (1983) 187.
[35] J. D. Talate, M. N. Desai and N. K. Shah, Anti-Corros. Meth. Mater. 52(2) (2009) 108.
[36] J. Rodosevic, M. Kliskic, L. J. Aijinovic and S. Vako, Proceeding of the 8th European Symposium on Corrosion Inhibitors, Ann Univ., Ferrara, N. S. Sez. V. Ferrara, Italy (1995) 817.
[37] B. Mernari, L. Elkadi and S. Kertit, Bull. Electrochem. 17(2001) 115.
[38] K. Arawaki, N. Hagiwara and H. Nishihara, Corros. Sci., 27(1987) 487.
[39] J. Marsh, Advanced Organic chemistry, Third ed., Wiely Eastern, Newdelhi, (1988).
[40] S. Martinz and I. Stern, Appl. Surf. Sci, 199(2002) 83.
[41] S. Kerte and B. Hammouti, Appl. Surf. Sci., 93(1996) 59.
[42] F. Bentiss, M. Traisnel and M. Lagrenee, Br. Corros. J., 35(2000) 315.
[43] S.S. Abd El-Rehim, H.H., Hassan and Amin M.A., Mater.Chem. Phys., 70(2001) 64
[44] A.K.Singh, M.A.Quraishi, Corros. Sci., 52(2010) 1373-1385
[45] F.Bentiss, C.Jama, B.Mernari, H. E.Attari, L. E.Kadi, M.Lebrini, M.Traisnel and M.Lagrenee, Corros. Sci., 51(2009)1628-1635
[46] M. Lagrenee, B. Mernari, B. Bouanis, M. Traisnel and F. Bentiss, Corros.Sci. 44(2002) 573.
[47] M. Bethencourt, F.J. Botana, J.J. Calvino, M. Marcos, Corros. Sci., 40(1998) 1803
[48] E. Kus, F. Mansfeld, Corros. Sci., 48(2006)

Publication History
Received 09th Sep 2014
Revised 16th Sep 2014
Accepted 15th Oct 2014
Online 30th Oct 2014